ARCHIVES OF ELECTRICAL ENGINEERING VOL. 68(1), pp. 209–220 (2019)

DOI 10.24425/aee.2019.125991

# Modelling of influence of mechanical stresses arising in magnetic circuit on magnetizing characteristic

**PAWEŁ IDZIAK, KRZYSZTOF KOWALSKI**

*Poznan University of Technology*
*Institute of Electrical Engineering and Electronics*
*ul. Piotrowo 3a, 60-965 Poznań, Poland*
*e-mails: {pawel.idziak/krzysztof.kowalski}@put.poznan.pl*

(Received: 30.09.2018; revised: 16.12.2018)

**Abstract:** An algorithm of determination of mechanical stresses and deformations of the magnetic circuit shape, caused by forces of magnetic origin, is presented in this paper. The mechanical stresses cause changes of magnetizing characteristics of the magnetic circuit. The mutual coupling of magnetic and mechanical fields was taken into account in the algorithm worked out. A computational experiment showed that it was possible to include the interaction of both fields into one numerical model. The elaborated algorithm, taking into account the impact of mechanical stresses on magnetic parameters of construction materials, can be used in both the 2D and the 3D type field-model.

**Key words:** modelling, coupled phenomena, magnetized characteristics, mechanical stress (MS)

## 1. Introduction

Processes occurring in electromagnetic transducers are conditioned by interaction of an electromagnetic field, mechanical phenomena (stress, shape deformation) and thermal phenomena. The majority of known publications consider the above-mentioned processes separately, without their interactions. In the publication [13], an attempt was made to connect chosen electromagnetic phenomena with mechanical ones. In the model proposed there, calculations are carried out serially, in two computing environments. The results of electromagnetic calculations are transmitted to the mechanical computing environment. A similar computational algorithm structure was described in the studies [1, 8].

In the present work, a coupled model of electromagnetic and mechanical phenomena is presented in a field-approach.

The object model should represent the phenomena occurring in a real object as precisely as possible. It is appropriate to introduce the simplifications reducing the computational complexity, but, at the same time, not influencing the results of calculations in any essential way. This is

particularly vital when using the finite element method, where the number of equations of the system to be solved may be amounted to several hundred thousand [12].

To determine the correctness of the adopted calculation process, a model of an electromagnetic circuit (choke) was elaborated, where both the nonlinearity of core magnetizing characteristics and coupled impact of mechanical stresses of electromagnetic origin on its course were taken into account. Then, the proposed calculation methodology was used to calculate the distribution of the magnetic field and mechanical stresses occurring in the circuit of a frameless direct current machine.

## 2. Description of the computational choke model

To represent the problem of calculations requiring the investigation of coupled phenomena, a demonstrative choke model with the air-gap and the winding fed with constant voltage was elaborated (Fig. 1).

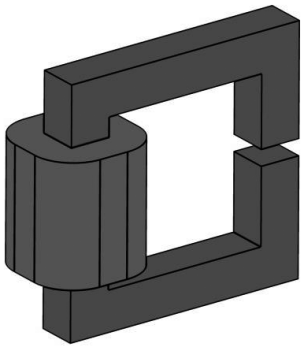

Fig. 1. Model of analysed circuit

The model geometry was elaborated in the commercial environment as a parameterized model. The two-dimensional model structure after automatic generation of digitizing net is shown in Fig. 2.

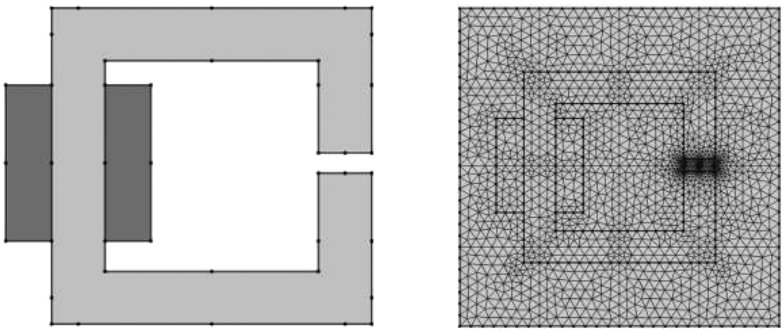

(a) (b)

Fig. 2. Analysed structure: (a) 2D model; (b) discretization of analysed area

The distribution of an electromagnetic field, slowly-variable in time, in a space containing soft ferromagnetic materials and areas with constant magnetic permeability, is described by the equations [3, 6, 9]:

$$\operatorname{curl}(\nu \operatorname{curl} \boldsymbol{A}) = \boldsymbol{J}, \tag{1}$$

$$\boldsymbol{J} = \gamma \left( \nabla V_e - \frac{\partial \boldsymbol{A}}{\partial t} \right), \tag{2}$$

where: $\nu$ is the magnetic reluctivity of the environment, $\boldsymbol{A}$ is the vector magnetic potential, $\boldsymbol{J}$ is the density vector of the conductivity current in subareas with electrical conductivity $\gamma$, $V_e$ is the scalar electrical potential.

The vector magnetic potential $\boldsymbol{A}$ appearing in Equation (1) is interrelated with the magnetic induction vector $\boldsymbol{B}$ by the dependence [3]:

$$\nabla \times \nu \nabla \times \boldsymbol{A} = \boldsymbol{J}, \tag{1a}$$

$$\boldsymbol{J} = \gamma \left( \nabla V_e - \frac{\partial \boldsymbol{A}}{\partial t} \right). \tag{2a}$$

It was admitted in the elaborated model that the magnetic properties of the soft ferromagnetic material are described by the relation [5, 6, 9]:

$$\boldsymbol{H} = \nu(|\boldsymbol{B}|)\,\boldsymbol{B}, \tag{3}$$

where: $\boldsymbol{H}$ is the magnetic intensity vector, $\nu(|\boldsymbol{B}|)$ is the magnetic reluctivity of the soft ferromagnetic material.

Boundary conditions of Dirichlet and Neuman determine then a unique solution of Equation (1).

For the considerations conducted in the orthogonal $xyz$ coordinate system and on the assumption that the $z$-axis will coincide with that of the machine shaft, field-magnitudes will be invariable along that axis in many cases. Such a simplification leads to calculations in a two or two and a half dimensional space. That last case will occur when one of the parameters is dependent on both space coordinates and the time. This leads then to equations in the following form:

$$\frac{1}{l}\left\{ \frac{\partial}{\partial x}\left( \nu \frac{\partial \phi}{\partial x} \right) + \frac{\partial}{\partial y}\left( \nu \frac{\partial \phi}{\partial y} \right) \right\} = -J, \tag{4}$$

$$J = \gamma \frac{\partial V_e}{\partial z} - \frac{\gamma}{l}\frac{\mathrm{d}\phi}{\mathrm{d}t}, \tag{5}$$

where: $\phi(t,\ x,\ y) = lA_z(t,\ x,\ y)$ represents the margin value of the potential $\boldsymbol{A}$, $A_z(t,\ x,\ y)$ stands for the component of the magnetic vector potential $\boldsymbol{A}$ in the $z$-axis direction, $l$ is the active length of elements of the machine magnetic circuit in the $z$-axis direction, $J$ is the component of the density vector of the conductivity current $\boldsymbol{J}$ in the $z$-axis direction.

This enables to determine both tangent and normal components of magnetic induction and consequently to describe mechanical stresses and deformations of a given structure.

In a three-dimensional orthogonal system, these deformations can be described by the following system of equations [7, 10]:

$$\varepsilon_x = \frac{\partial u}{\partial x}, \qquad \varepsilon_{xy} = \frac{\gamma_{xy}}{2} = \frac{1}{2}\left( \frac{\partial u}{\partial y} + \frac{\partial u}{\partial x} \right), \tag{6a}$$

$$\varepsilon_y = \frac{\partial u}{\partial y}, \qquad \varepsilon_{yz} = \frac{\gamma_{yz}}{2} = \frac{1}{2}\left(\frac{\partial u}{\partial z} + \frac{\partial u}{\partial y}\right), \tag{6b}$$

$$\varepsilon_z = \frac{\partial u}{\partial z}, \qquad \varepsilon_{xz} = \frac{\gamma_{xz}}{2} = \frac{1}{2}\left(\frac{\partial u}{\partial z} + \frac{\partial u}{\partial x}\right), \tag{6c}$$

where: $\varepsilon_x$, $\varepsilon_y$, $\varepsilon_z$ are the deformations in $x$, $y$, $z$ direction correspondingly.

On the basis of deformation values and the knowledge of the elasticity matrix $\boldsymbol{D}$, the matrix of normal and tangent tensions $\boldsymbol{\sigma}$ can be determined:

$$\boldsymbol{\sigma} = \boldsymbol{D}\boldsymbol{\varepsilon}, \tag{7}$$

where:

$$\boldsymbol{\sigma} = \begin{bmatrix} \sigma_x \\ \sigma_y \\ \sigma_z \\ \tau_{xy} \\ \tau_{yz} \\ \tau_{xz} \end{bmatrix}, \qquad \boldsymbol{\varepsilon} = \begin{bmatrix} \varepsilon_x \\ \varepsilon_y \\ \varepsilon_z \\ \varepsilon_{xy} \\ \varepsilon_{yz} \\ \varepsilon_{xz} \end{bmatrix}. \tag{8}$$

The elasticity matrix $\boldsymbol{D}$ is defined as follows:

$$\boldsymbol{D} = \frac{E}{(1+\nu_p)(1-2\nu_p)} \begin{bmatrix} 1-\nu_p & \nu_p & \nu_p & 0 & 0 & 0 \\ \nu_p & 1-\nu_p & \nu_p & 0 & 0 & 0 \\ \nu_p & \nu_p & 1-\nu_p & 0 & 0 & 0 \\ 0 & 0 & 0 & \dfrac{1-2\nu_p}{2} & 0 & 0 \\ 0 & 0 & 0 & 0 & \dfrac{1-2\nu_p}{2} & 0 \\ 0 & 0 & 0 & 0 & 0 & \dfrac{1-2\nu_p}{2} \end{bmatrix}, \tag{9}$$

where: $E$ means the rigidity coefficient (Young's module), and $\nu$ is the Poisson ratio.

For linear systems, i.e. those deformed within the elasticity range, the Navier equation remains valid. After taking into account the mass and material parameters of the structure elements, it enables to determine their specific values.

The system of equations describing the considered model was solved by using a commercial computing environment (solver). Calculations were carried out on the assumption that the magnetic circuit was made of electrical sheet metal with magnetizing characteristics shown in Fig. 3. It was admitted that the considered structure was fastened to the ground along the external plane surface of the left limb (Fig. 4).

According to the literature [4, 11], mechanical stresses within the range of elastic deformations that appear in a magnetic circuit, cause changes in the course of magnetizing characteristics. For small tensile stresses, the steepness of the characteristics $B(H)$ is increased in its initial part. In calculations to be carried out, the impact of stresses on the induction value was taken into account by means of the correcting coefficient $w_k$. The value of this coefficient for the assumed characteristics of the magnetization, has been determined in accordance with guidelines specified in [2]. The algorithm of the proposed calculations is shown in Fig. 5. Completion of the iteration occurs when the error value $\xi$ of the calculation is equal to or less than the acceptable error $\xi_0$ imposed by the user.

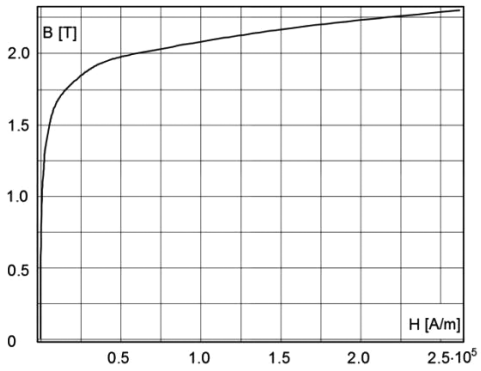


Fig. 3. Magnetizing characteristics of core material

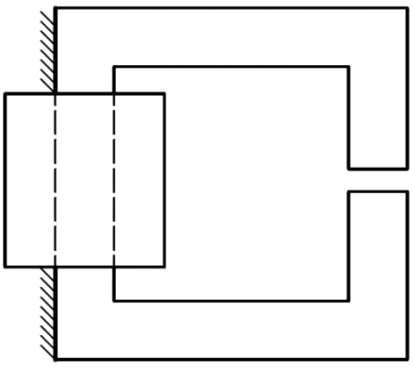

Fig. 4. Fastening of the limb to the ground

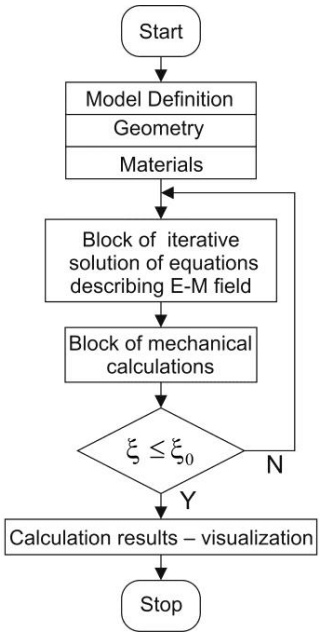


Fig. 5. Block diagram of coupled calculation algorithm

## 3. Calculation results

Distributions of magnetic induction in the core and stress distributions are the result of calculations. The computational experiment was carried out for a fixed value of the current feeding the winding in two cases:

a) without taking into account the impact of stresses on the characteristics $B(H)$ (the so-called direct coupling [8]),

b) taking into account the interactions of both electromagnetic and mechanical fields (bidirectional coupling [8]).

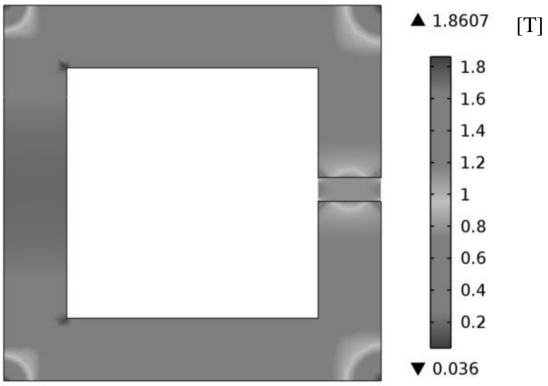


Fig. 6. Distribution of magnetic induction in the core without taking into account the impact of mechanical stresses

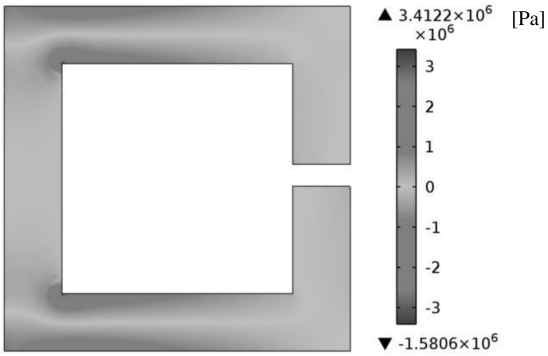


Fig. 7. Distribution of mechanical stresses in the core for direct coupling

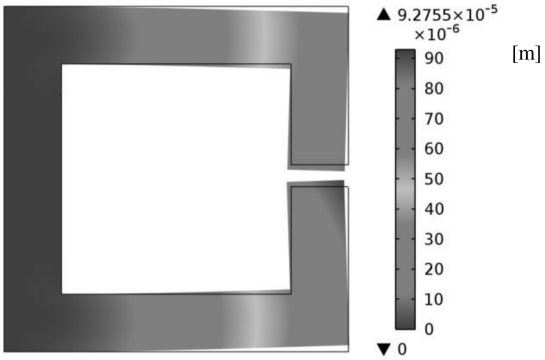


Fig. 8. Elastic deformations of the core caused by electromagnetic forces for direct coupling (zoom scale $4 \cdot 10^5$)

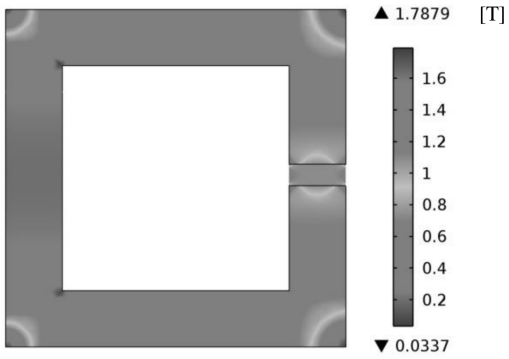


Fig. 9. Distribution of magnetic induction in the core, taking into account the impact of mechanical stresses

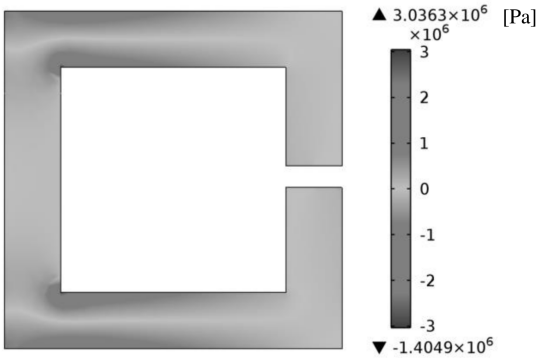


Fig. 10. Distribution of mechanical stresses in the core, taking into account the interactions of both electromagnetic and mechanical fields

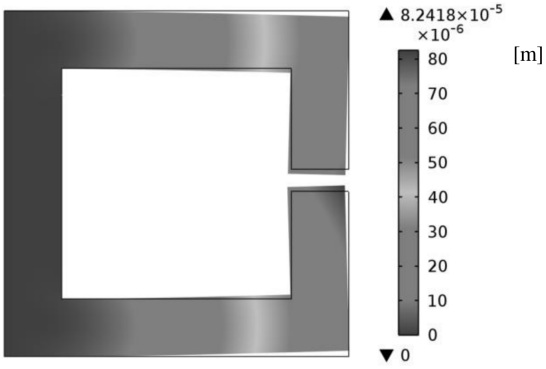


Fig. 11. Elastic deformations of the core caused by electromagnetic forces, taking into account the interactions of both electromagnetic and mechanical fields (zoom scale $4 \cdot 10^5$)

The numerical experiment showed that taking into account the impact of mechanical stresses on the magnetizing characteristics did not result in significant change of the distribution of magnetic induction in the core. However, the maximum value of the induction was reduced by approximately 4%.

The calculation of the mechanical stresses showed that their maximum value for direct coupling was higher by approximately 11% than that for bidirectional one.

## 4. Numerical model of a direct current machine and calculation results

The computational experiment was carried out for the magnetic circuit of a currently produced G series direct current machine with a power of 3 kW. This is a frameless machine.

It has been assumed in the calculations that the magnetic circuit of the machine was made of EP 350-50A type electrical sheet metal. After the blanking process, the sheet metal was not subjected to any annealing process.

No account of magnetostriction phenomena was taken for numerical calculations. Both an armature current and excitation one were taken into account. The model presented here has more than 200 thousand nodes (Fig. 12).

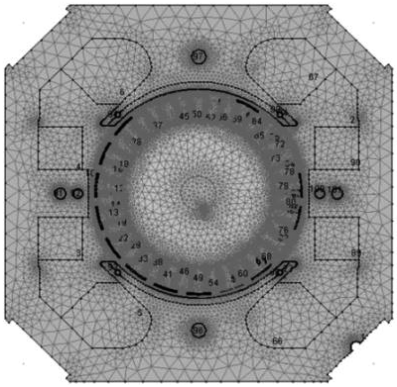

Fig. 12. Digitalization net of the stator and rotor magnetic circuit of modelled frameless direct current machine

The computational experiment consisting in determination of the magnetic field distribution, i.e. in determination of the course of field force lines and of the magnetic induction vector values in the magnetic circuit area and in that of the air-gap, was carried out for cases, where:

– material magnetizing characteristics determined for a 500 mm wide sheet metal band was used in calculations (the size corresponding to that of samples used for the 50 cm Epstein apparatus), without taking into account the impact of occurring mechanical stresses caused by electromagnetic forces,
– locally occurring stresses due to stresses caused by the above-mentioned electromagnetic forces were taken into account.

The calculations were carried out for a steady state, i.e. it was assumed that the windings were fed with a preset (fixed) value of a direct current (without any variable component), the rotor was immobile – the calculations pertain to a specific time point.

Examples of calculation results are provided in Figs. 13–17.

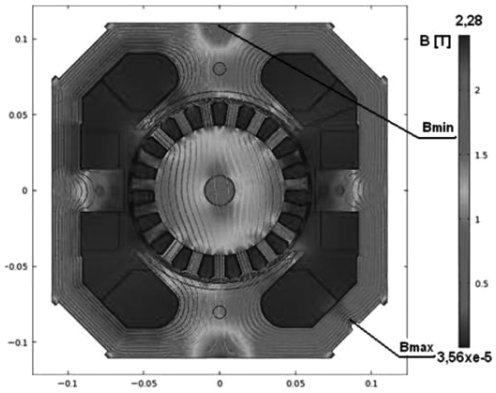


Fig. 13. Distribution of magnetic induction and magnetic field force lines in the examined machine, determined on the assumption that the magnetizing characteristics of a 500 mm wide sheet metal band is valid for the entire structure

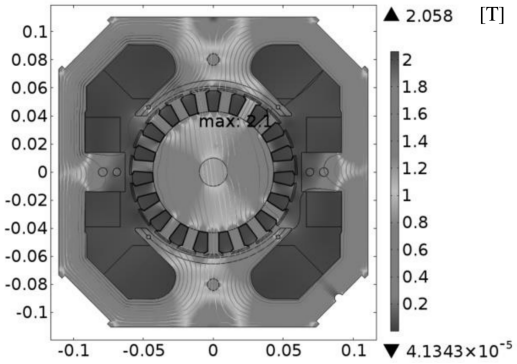


Fig. 14. Distribution of magnetic induction and magnetic field force lines in the examined machine without taking into account the impact of stresses on the characteristics $B(H)$ (direct coupling)

The observed changes of induction and stress values, caused by a different way of coupling of both effects are similar to those for the choke (6% – for the induction, 13% for maximum values of mechanical stresses).

The distribution of magnetic induction in the air gap of the machine for both considered cases is shown in Fig. 18.

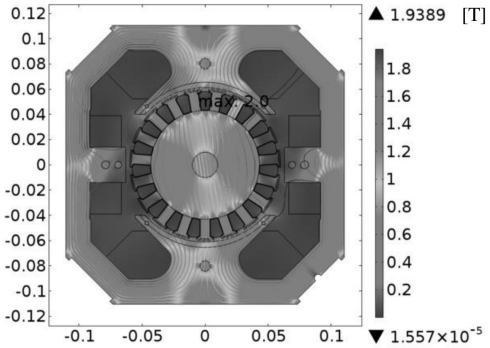


Fig. 15. Distribution of magnetic induction and magnetic field force lines in the examined machine, taking into account the interactions of both electromagnetic and mechanical fields (bidirectional coupling)

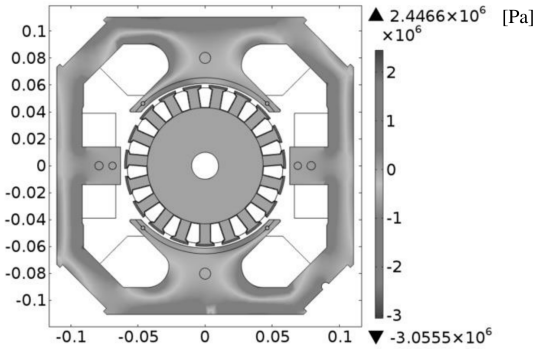


Fig. 16. Distribution of mechanical stresses in the examined machine without taking into account the impact of stresses on the characteristics $B(H)$ (direct coupling)

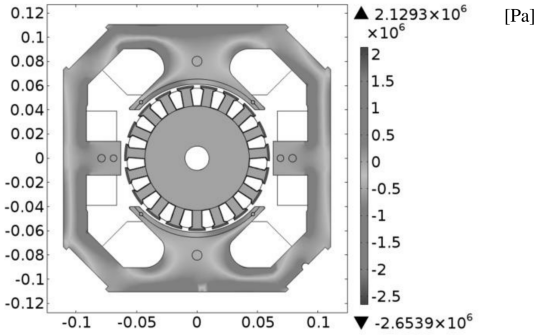


Fig. 17. Distribution of mechanical stresses in the examined machine, taking into account the interactions of both electromagnetic and mechanical fields (bidirectional coupling)

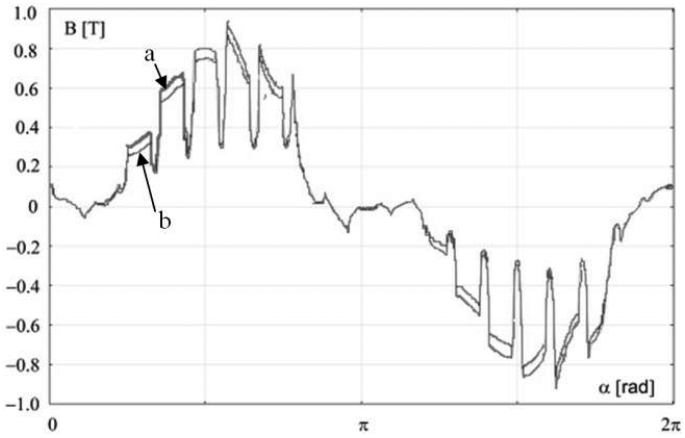


Fig. 18. Distribution of magnetic induction in the air gap of a direct current machine, determined for the case of: "a" – direct coupling; "b" – interaction of both fields taken into consideration

## 5. Summary

The computational experiment for elaborated models showed the possibility of execution of calculations, taking into account the mutually coupled effect of both electromagnetic and mechanical fields. The calculation results showed that, in spite of considerable local stress values, elastic deformations of the structure were small, so that the changes in the shape of the magnetic circuit had a negligible effect on the operating point of the magnetic circuit. The use of deformations for the determination of the correction coefficient value is not necessary. The methodology that takes into account the interaction between the stress value and the change in the course of magnetizing characteristics, elaborated by the authors, can be used to the analysis of both two-dimensional and three-dimensional systems.

**References**

[1] Antczak M., Idziak P., *The influence of the sheet punching on the magnetic field distribution in a dc machine*, Przeglad Elektrotechniczny (in Polish), no. 4a, pp. 6–9 (2012).

[2] Bielow K.P., *Phenomena in magnetic materials*, PWN (in Polish), Warszawa (1962).

[3] Biro O., Richter K., *CAD in electromagnetism*, Advances in electronics and electron physics, vol. 82, pp. 1–96 (1991).

[4] Cichy J., Dąbrowski M., *Magnetic properties of structural steel*, Archives of Electrical Engineering (in Polish), vol. XXIV, no. 2, pp. 329–343 (1975).

[5] Dąbrowski M., Demenko A., Szeląg W., *Hybrid method of determining the magnetic field in permanent magnet circuits*, Rozprawy Elektrotechniczne (in Polish), no. 2, pp. 621–635 (1986).

[6] Demenko A., *Circuits models of systems with an electromagnetic field*, Wydawnictwo Politechniki Poznańskiej (in Polish), Poznań (2004).

[7] den Hartog J.P., *Mechanical Vibrations*, McGraw Hill Book Company, fourth edition (1965).

[8] Hameyer K., Böhmer S., Coenen I., Eggers D., Felden M., Franck D., Hafner M., Henrotte F., Herold T., Hombitzer M., Lange E., Offermann P., Riemer B., Steentjes S., *The art of Electrical Machine*, ICS Newsletter, International Compumag Society, vol. 19, no. 2, ISSN 1026-0854, pp. 3–19 (2012).

[9] Szeląg W., *Field approach to the analysis and design of permanent magnet synchronous motors*, Wydawnictwo Politechniki Poznańskiej (in Polish), Poznań (1998).

[10] Timoschenko S., *Vibration problems in engineering*, D. Van Nostrand Company, Inc, Princeton, New Jersey, Toronto, New York (1956).

[11] Wilczyński W., *The influence of technological operations on the magnetic properties of electric motor core*, Wydawnictwo Instytutu Elektrotechniki w Warszawie (in Polish), Warszawa (2003).

[12] Zienkiewicz O., Taylor T., *The Finite Element Method*, McGraw-Hill Book Company (1989).

[13] Żurek Z.H., Śladowski M., *Influence of stress in interference joint between frame and stator on flux density distribution in the air gap*, Zeszyty Problemowe – Maszyny Elektryczne (in Polish), BOBRME Komel, no. 85, pp. 167–171 (2010).